

Dielectric and viscoelastic properties of KNbO₃ doped BaTiO₃Liang Dong,¹ Donald S. Stone,² and Roderic S. Lakes^{1,2,3,a)}¹*Department of Engineering Physics, University of Wisconsin, Madison, Wisconsin 53706-1687, USA*²*Materials Science Program, University of Wisconsin, Madison, Wisconsin 53706-1687, USA*³*Engineering Mechanics Program, University of Wisconsin, Madison, Wisconsin 53706-1687, USA*

(Received 17 October 2010; accepted 24 December 2010; published online 28 March 2011)

Fine grain (1–2 μm) 2%, 3% KNbO₃-BaTiO₃ ceramics have been synthesized via the solid state reaction method. Fine and coarse grain ceramics sintered at different temperatures exhibit peaks in dielectric constant and internal friction in the vicinity of transition temperatures. Doping lowered the Curie point and raised the temperatures for the structural transformations between orthorhombic and rhombohedral symmetry and broadened the response near the transformations. Dielectric and viscoelastic responses sharpened with increasing sintering cycles. This effect is attributed to a reduced core-shell effect. Doped ceramic exhibited a relaxation peak due to oxygen vacancy with a similar activation energy and relaxation time as pure material. The steep increase in dielectric constant and internal friction in the ferroelectric phase and the reduced dielectric and mechanical anomaly in the vicinity of the transformations in the fine grain ceramics are attributed to the internal stress built up at the grain boundaries. Other possible mechanisms involved such as oxygen vacancy pinning effect, constrained negative stiffness 90° domain bands and the liquid phase effect have also been discussed. © 2011 American Institute of Physics. [doi:10.1063/1.3552600]

I. INTRODUCTION

Ferroelectric materials such as barium titanate are of interest in the context of ceramic capacitors and piezoelectric transducers. These materials typically exhibit several phase transformations; above the Curie point, the crystal symmetry becomes insufficient for piezoelectricity. Pure barium titanate has lower piezoelectric sensitivity than lead titanate zirconate. However, doped barium titanate can exhibit competitive piezoelectricity with the benefit of being lead free. Addition of dopants shifts the phase transformation temperatures; in particular, the Curie point is shifted to a lower temperature. Although this is a drawback for high temperature applications, the increased ambient temperature properties could be beneficial for applications of piezoelectric materials where service temperature is moderate. Extensive studies have been performed on the piezoelectric and dielectric properties of barium titanate based ceramics. Recently, such a well-known material has been found to possess negative bulk stiffness during the phase transformation near the Curie point.^{1,2} Such a property has been utilized to fabricate composite materials with ultra high damping and stiffness.³ Yet real application of such composite materials requires the capability to tune the activation temperature for the negative stiffness behavior of the inclusion. Therefore the shifting of the Curie point in doped barium titanate ceramic shed a light on both electrical and mechanical applications. This paper deals with electrical and mechanical properties of BaTiO₃ doped with KNbO₃ and their relation to composition heterogeneity and microstructure.

II. SYNTHESIS METHOD

The ceramic was synthesized by means of the solid state reaction method. The procedure is adapted from the method outlined by Avrahami.⁴ KNbO₃ (Alfa Aesar, Puratronic[®], 99.999% metal basis) and BaTiO₃ (Alfa Aesar, 99.7% metal basis) powders were used as precursors. Powders with the desired molar ratio were mixed and ball milled in a silicon nitride vial for 25–30 min with a high energy milling machine (SPEX SamplePrep 8000M Mill/Mixer; 115V 60Hz, SPEX CertiPrep, Metuchen, NJ). The 3644 Ultrabind binder (SPEX CertiPrep PrepAid, Metuchen, NJ) was then added into the vial and mixed another 3 min to allow the binder to evenly spread in the precursor powders. Powders were then transferred into a specially designed stainless steel compression mold with diameter of 28.5 mm, and a uniaxial pressure up to 110 MPa was applied using a hydraulic press (Carver hydraulic laboratory pellet press, SPEX SamplePrep 3621 Carver[®] model C, Metuchen, NJ) of capacity of 24 000 lb at room temperature. The green pellet has a typical dimensions of $\phi 28.5 \times 5$ mm. Solid state reaction was performed in air at 800 °C for 4 h, followed by sintering (at atmospheric pressure) in air at either 1300 or 1400 °C for 10–15 h. To facilitate composition homogeneity, additional ball milling and sintering steps were performed with the same procedures as the first. From the first to the sixth sintering cycles, binder was added 10–15% by weight. The final densities of these ceramics are about 75–85% of the theoretical density. For the ninth cycle, only 2% binder by weight was added. A reduction in binder increases the final density (there is less porosity) at the expense of a more friable green pellet. The density of the ceramic sintered nine times is about 95% of the theoretical value. A ramp up rate of 3 °C/min was applied. Each sample was then cooled to ambient

^{a)}Author to whom correspondence should be addressed. Electronic mail: lakes@engr.wisc.edu.

temperature with a rate of $4^{\circ}\text{C}/\text{min}$. Samples were kept inside an alumina crucible with an alumina lid on top so as to avoid possible contamination from any residue left inside the furnace. To avoid reaction between sample and the crucible, samples were buried inside pure BaTiO_3 powders. Optical microscopy showed an average grain size of $1\text{--}2\ \mu\text{m}$ for the KNbO_3 doped BaTiO_3 .

III. CHARACTERIZATION METHODS

Dielectric measurements were performed with a simple bridge circuit. A sample with a typical size of $4 \times 5 \times 1.3\ \text{mm}^3$ was coated with conductive electrodes by gold sputtering and connected in series with a capacitor of $1000\ \text{pF}$. A lock-in amplifier (Stanford Research System SR 850) served as both signal generator (at $10\ \text{kHz}$) and receiver. The temperature range assumed was from -20 to 150°C . A thermal rate of $0.03^{\circ}\text{C}/\text{s}$ was applied during measurements.

Mechanical properties (internal friction, shear, and Young's moduli) were studied via broadband viscoelastic spectroscopy.⁵ Specimens with typical size of $1 \times 2 \times 15\ \text{mm}^3$ were cut with a low speed diamond saw. The specimens were not subjected to electrical poling. Deformation of the specimens was induced by a permanent magnet attached at one end of the specimen activated by magnetic coils and measured by a laser light method. Bending was performed to obtain the complex Young's modulus, and torsion was performed to obtain the complex shear modulus. Frequency range accessed was 0.1 to $100\ \text{Hz}$ (below the lowest natural frequency: $\sim 750\ \text{Hz}$ in bending; $\sim 8000\ \text{Hz}$ in torsion). The maximum surface strain was on the order of 3×10^{-5} . Internal friction was determined as $\tan \delta$, with δ as the phase angle between stress and strain. Bulk modulus was inferred via the elastic interrelation for isotropic materials. Data were captured by a lock-in amplifier (Stanford Research System SR850). Temperature was monitored by a thermocouple (OMEGA L-0044 K type) $1\ \text{mm}$ away from the specimen surface in both dielectric and viscoelastic measurements.

IV. RESULTS AND DISCUSSION

The effect of sintering cycles is shown in Fig. 1, which shows the change in dielectric constant of 2% $\text{KNbO}_3\text{-BaTiO}_3$ over multiple sintering cycles. Clearly, the dielectric peak at the phase transformation temperatures becomes sharper with the number of sintering cycles, but the doped material never exhibits as sharp a response as pure barium titanate. After the first sintering step, the signature of the Curie point of the pure BaTiO_3 is still visible near 130°C . Also the two transformations (cubic-tetragonal and tetragonal-orthorhombic) are closer to each other. The baseline difference could come from the density variation due to the amount of binder used. The specimen that has been sintered for nine times has a higher density (about 95% theoretical density) than the other ones. The baseline moves up, and the absolute peak magnitude (relative to baseline) near the Curie point is higher compared with the lower density ceramics. This is attributed to the space charge field inside the ceramic. For a dense ceramic, the charge field can be more easily removed

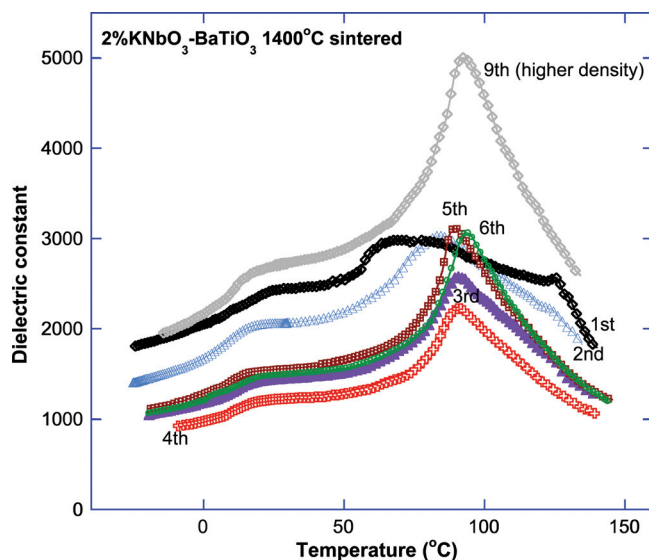


FIG. 1. (Color online) Dielectric behaviors at $10\ \text{kHz}$ of 2% $\text{KNbO}_3\text{-BaTiO}_3$ over multiple sintering cycles. Sintering was performed at 1400°C for $15\ \text{h}$ for each cycle. Grain size for each specimen is about $1\text{--}2\ \mu\text{m}$.

by the charge of the surrounding grains compared with a porous grain ceramic.⁶ Also composition homogeneity will promote dielectric response in the vicinity of the Curie point. This effect can be appreciated by the fact that the specimen sintered five times exhibited a much higher dielectric constant near the Curie point but has similar dielectric responses near the orthorhombic-tetragonal transition and in both ferroelectric and paraelectric states compared with the specimen sintered three times. Such an effect has also been observed in 3% $\text{KNbO}_3\text{-BaTiO}_3$, as in Fig. 2(b).

The effect of grain size (due to processing difference) upon dielectric constant is shown in Fig. 2. Dielectric constant is plotted vs temperature for fine grain ($1\text{--}2\ \mu\text{m}$) 2% and 3% $\text{KNbO}_3\text{-BaTiO}_3$ after at least four sintering cycles. Behavior of coarse grain ($15\ \mu\text{m}$ on average) 3% $\text{KNbO}_3\text{-BaTiO}_3$ (Ref. 7) has been compared. This coarse grain 3% $\text{KNbO}_3\text{-BaTiO}_3$ (Ref. 7) has experienced three sintering cycles (about 1325°C for $15\ \text{h}$ for each cycle) and has a density near 90% of theoretical. The final large grain size is attributed to the smaller particle size of the initial powders (ball milling was performed $2\ \text{h}$ in that study) as surface energy is the driving force for grain growth during sintering. The tetragonal-orthorhombic transformation temperature of the fine grain 3% $\text{KNbO}_3\text{-BaTiO}_3$ is higher than coarse grain ceramic while the Curie point basically has no shift. The dielectric constant is higher in fine grain ceramic in the ferroelectric phase, whereas it is almost independent of grain size in the paraelectric phase. Such behaviors are consistent with pure BaTiO_3 with decreasing grain size when the grain size is $<10\ \mu\text{m}$ ^{8,9} (the dielectric constant is independent of grain size in pure BaTiO_3 when grain size $>10\ \mu\text{m}$). The 3% $\text{KNbO}_3\text{-BaTiO}_3$ has lower transformation temperatures but higher dielectric constant values than 2% $\text{KNbO}_3\text{-BaTiO}_3$ with similar grain size and density. This figure also presents the dielectric behaviors of pure BaTiO_3 sintered at 1400°C for $8\ \text{h}$ (prepared in the present study). However, the pure BaTiO_3 has an average grain size about $15\ \mu\text{m}$.

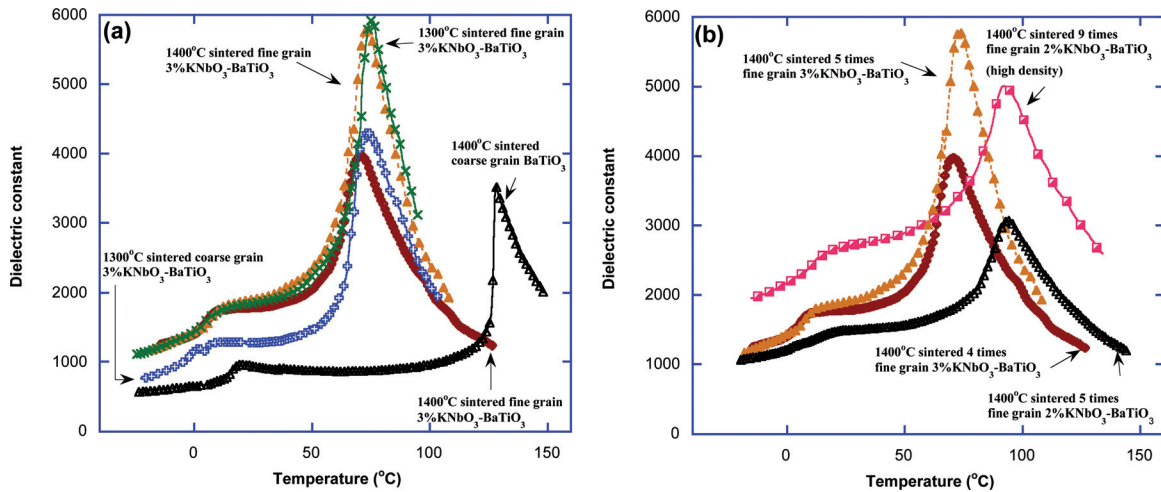


FIG. 2. (Color online) (a) Dielectric constants of fine grain ($1\text{--}2\ \mu\text{m}$) and coarse grain ($15\ \mu\text{m}$) $3\% \text{KNbO}_3\text{-BaTiO}_3$ and coarse grain ($15\ \mu\text{m}$) pure BaTiO_3 . This coarse grain $3\% \text{KNbO}_3\text{-BaTiO}_3$ was studied in Ref. 7. The two 1400°C sintered fine grain $3\% \text{KNbO}_3\text{-BaTiO}_3$ samples came from different pieces with comparable grain size and density. The one with a higher dielectric constant near the Curie point was sintered five times, whereas the other was sintered four times. The 1300°C sintered fine grain $3\% \text{KNbO}_3\text{-BaTiO}_3$ has experienced five sintering cycles. (b) Dielectric constants of 1400°C sintered fine grain ($1\text{--}2\ \mu\text{m}$) 2% (the same samples as shown in Fig. 1) and 3% [the same samples as shown in Fig. 2(a)] $\text{KNbO}_3\text{-BaTiO}_3$.

A phase diagram of the $\text{KNbO}_3\text{-BaTiO}_3$ system based upon our present and previous⁷ results is shown in Fig. 3. The temperatures at which peaks occur in dielectric, thermal, and internal friction properties are all similar as shown by the points in the diagram. Phase boundaries (thick dash lines) are drawn based on these points. These boundaries, particularly for the tetragonal-orthorhombic and orthorhombic-rhombohedral transitions, differ from those of Bratton.¹⁰ However, Bratton used a dielectric method on ceramics sintered a few times, which generated broad peaks more than 50°C wide.

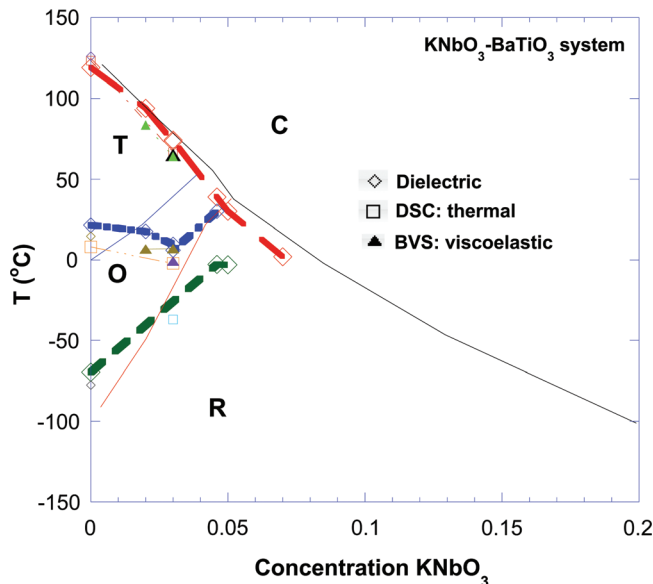


FIG. 3. (Color online) Phase diagram for the $\text{KNbO}_3\text{-BaTiO}_3$ system. Thin solid lines are after dielectric measurements of Bratton's work (Ref. 10). Points include results of the present measurements and points obtained from our previous study (Ref. 7) on the coarse grain $3\% \text{KNbO}_3\text{-BaTiO}_3$. Dielectric data points for pure fine grain BaTiO_3 come from Ref. 8. Thick dash lines are from the present study on fine grain 2, 3, 4.6, 5, and $7\% \text{KNbO}_3\text{-BaTiO}_3$. The coarse grain ceramic has lower rhombohedral-orthorhombic and orthorhombic-tetragonal transition temperatures but similar Curie point compared to the fine grain ceramic. (C: Cubic; T: Tetragonal; O: Orthorhombic; R: Rhombohedral).

The phase boundaries in Bratton's study are therefore uncertain. In the present study, the transition temperatures can be easily determined at lower concentration ($< 3\% \text{KNbO}_3$) but become much more difficult to be determined at higher concentration due to the weak and broad responses in the dielectric, thermal, and mechanical properties. Viscoelastic spectroscopy discloses sharper peaks than dielectric measurements. Moreover the processing is different in that more sintering steps were done in the present study.

The dielectric constant (Fig. 4) follows the Curie-Weiss law in the paraelectric phase when $T \gg T_C$. The Curie point

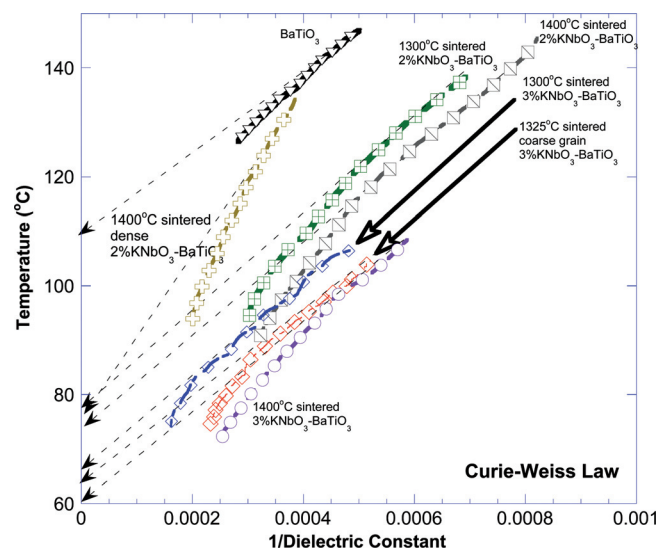


FIG. 4. (Color online) Curie-Weiss plot to determine the Curie temperatures and Curie constants. The Curie-Weiss law is written $k = C_0/(T - T_0)$, in which k , C_0 , and T_0 represent dielectric constant, Curie constant, and Curie temperature, respectively. Curie temperature is determined as the intercept of the tangent line of curve $T = T_0 + C_0/k$ on the T axis ($T \gg T_C$), and the Curie constant is the slope of this tangent line. Unless specified, the doped barium titanate samples are fine grain. The dash arrow lines are the tangent lines for the curves. Intercepts of these dash arrow lines on the temperature axis correspond to the Curie temperatures, while the slopes of these lines correspond to the Curie constants.

TABLE I. Summary of Curie point (T_C), Curie temperature (T_0), and Curie constant (C_0) of KNbO_3 doped BaTiO_3 prepared in the present study. A comparison has been given with coarse grain 3% KNbO_3 - BaTiO_3 , (Ref. 7) coarse grain pure BaTiO_3 ($\sim 70\%$ theoretical density), and pure BaTiO_3 (1000°C sintered with average grain size distribution from 1.1 to $53\ \mu\text{m}$) (Ref. 8) Temperatures given in the table indicate the sintering temperatures, % represents the KNbO_3 concentration. Unless specified, samples are fine grain and 75–85% theoretical density. The dense 1400°C sintered fine grain 2% KNbO_3 - BaTiO_3 is about 95% theoretical density.

	1300 °C 2%	1400 °C 2%	1400 °C 2% Dense	1300 °C 3%	1400 °C 3%	1325 °C 3% Coarse Grain	1400 °C 0% Coarse Grain	1000 °C 0% ^a
T_0 (°C)	78	74	76	66	61	64	110	108–113
T_C (°C)	94	91	93	74	73	74	127	120–122
ΔT ($T_C - T_0$) (°C)	16	17	17	8	12	10	17	8–14
C_0 (°C)	86 000	82 000	147 000	88 000	84 000	79 000	74 000	123 000–167 000

^aReference 8.

(T_C), Curie temperature (T_0), and Curie constant (C_0) of the ceramics prepared in the present study have been summarized in Table I. The Curie point is higher in the ceramic sintered at lower temperature (1300°C). Divergence between Curie point and Curie temperature is an indication of the order of phase transition. If $T_C = T_0$, transition is second order; if $T_C > T_0$, transition is first order.¹¹ Yet the difference between T_C and T_0 is basically independent of grain size and density but shows a trend of slight decrease with increasing dopant concentration and decreasing sintering temperature. Fine grain ceramic has higher C_0 than coarse grain ceramic. C_0 is much higher in dense ceramic.

Figure 5(a) presents the internal friction spectrum of fine grain (1–2 μm) 2%, 3% KNbO_3 - BaTiO_3 (1400°C sintered) and coarse grain (15 μm) 3% KNbO_3 - BaTiO_3 ceramic.⁷ An excitation frequency of 10 Hz and a thermal rate of 0.035°C/s were applied. The fine grain ceramic exhibited a much broader internal friction peak near the transition temperatures in comparison with the coarse grain ceramic of the same composition. The orthorhombic-tetragonal transition temperature shift is apparent when grain size decreases. The internal friction during the transformation has three contributions (Ref. 12): transient term, phase transition itself, and intrinsic term. The transient component is attributed to the moving of phase interface (because the transformation fol-

lows nucleation and growth mechanism) and is the main contribution to the internal friction spectrum if not in an isothermal or quasi-isothermal condition; the second term is attributed to the vibration of the phase interface and only contributes considerably at a driving frequency of kHz. The third term depends on the microstructures of both parent and new phases and merely serves as the baseline.

It is worth mentioning that the fine grain KNbO_3 doped BaTiO_3 ceramic also presents a relaxation peak in the tetragonal phase, which has been observed in pure BaTiO_3 attributed to the motion of oxygen vacancy (V_O) under external stress.¹³ Figure 6 presents the frequency dependent internal friction spectrum for the fine grain 2% and 3% KNbO_3 - BaTiO_3 in the tetragonal phase. Activation energy and relaxation time for such a relaxation process have been calculated according to the Arrhenius equation. Such a relaxation peak has approximately the same activation energy and relaxation time, indicating the same mechanism for this peak in both samples. A secondary peak of this type has been observed in tetragonal BaTiO_3 in our previous study.¹⁴

Based upon the relationship of domain size and grain size of barium titanate,⁹ a grain size about 1–2 μm has a domain size about 0.15 μm . The grain size is about 25 μm , and domain size is about 1 μm in that study and a relaxation time about 8×10^{-12} s and activation energy about 0.8 eV were

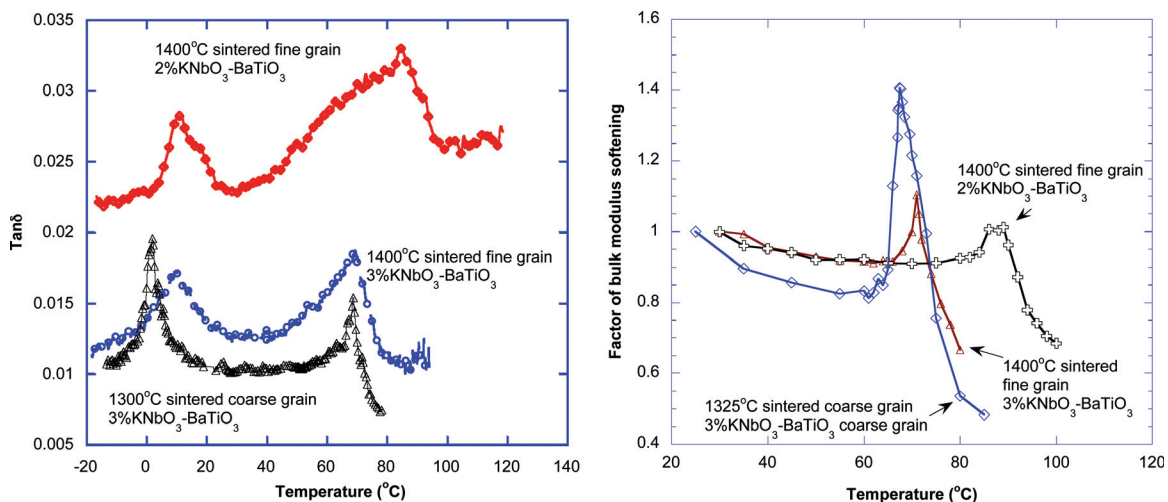


FIG. 5. (Color online) (a) Internal friction $\tan\delta$ of fine grain (1–2 μm) 2% KNbO_3 - BaTiO_3 ($\sim 95\%$ density) and 3% KNbO_3 - BaTiO_3 ($\sim 85\%$ density) and coarse grain (15 μm) 3% KNbO_3 - BaTiO_3 ($\sim 90\%$ density). Excitation frequency of 10 Hz was applied. Thermal rate was about 0.035°C/s (left); (b) Magnitude of bulk modulus softening vs temperature of 1400°C sintered fine grain 2% ($\sim 95\%$ density), 3% KNbO_3 - BaTiO_3 ($\sim 85\%$ density), and coarse grain 3% KNbO_3 - BaTiO_3 ($\sim 90\%$ density), normalized by ambient temperature moduli values. Tests were performed at 0.1 Hz driving frequency in quasi-isothermal condition (0.008°C/s) (right).

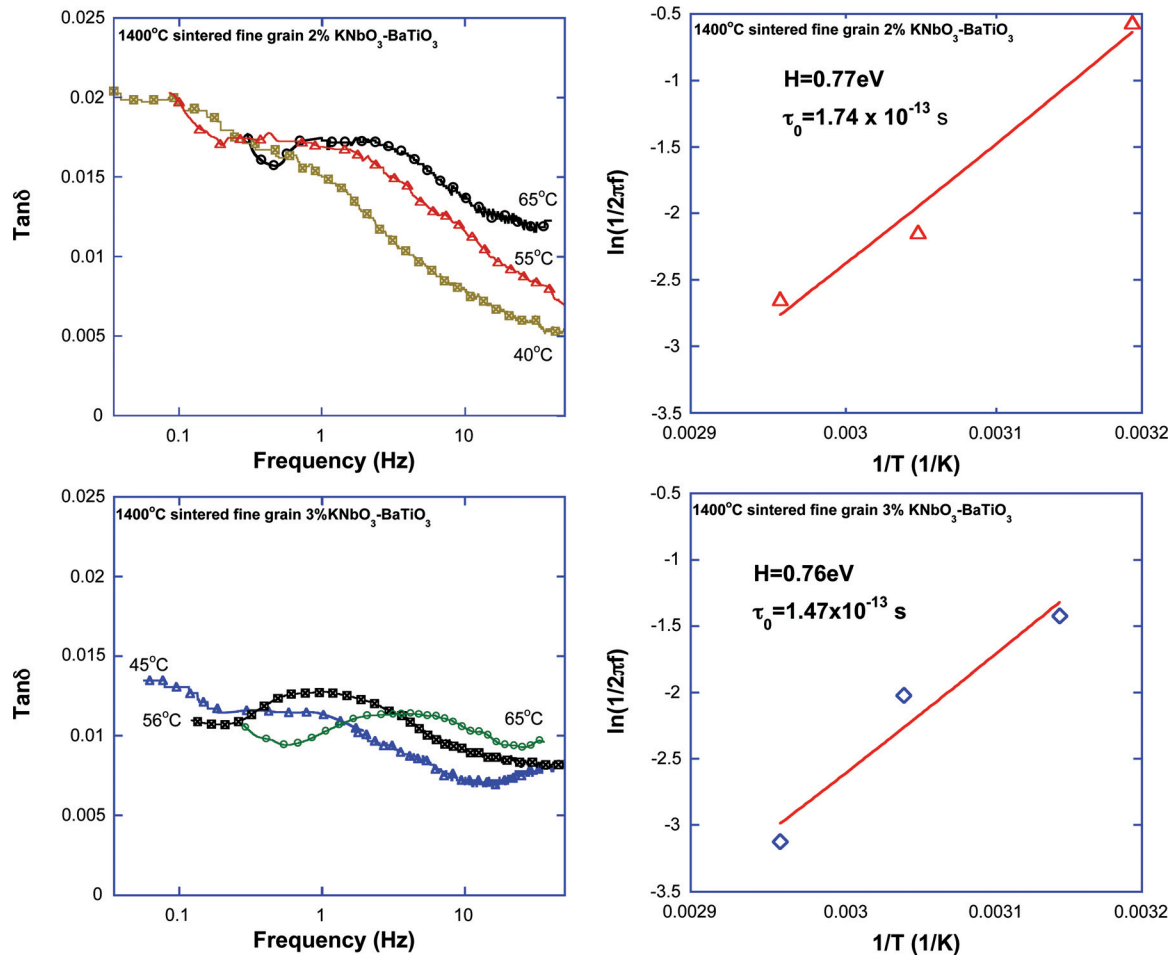


FIG. 6. (Color online) Frequency dependent internal friction spectrum at different temperatures in the tetragonal phase of the fine grain 2% KNbO₃-BaTiO₃ (~95% theoretical density) and 3% KNbO₃-BaTiO₃ (~85% theoretical density). Both ceramic samples were sintered at 1400 °C. A relaxation peak is observed in both ceramic samples. Activation energy H and relaxation time τ have been calculated as shown inset.

found. According to the relationship between relaxation time and domain width:¹⁵

$$\tau = L^2 / (\pi^2 D),$$

where D is diffusion coefficient, a domain size about 0.15 μm will give a relaxation time about 1.8×10^{-13} s, which agrees well with the relaxation time of the secondary peak observed in the present study. However, the magnitude of such peak depends on V_{O} concentration. V_{O} has certain pinning effect on the domain wall, and this will weaken the elastic softening during phase transformations. Contribution of domain wall moving to elastic softening near the Curie point will be illustrated later.

Internal stress will be introduced when the ceramic transforms from paraelectric state into ferroelectric state. Generating 90° domains is the most effective way to release this internal stress. In coarse grain ($>10 \mu\text{m}$) ceramic, such stress can be easily released by developing 90° domains with multiple configurations. However, in fine grain (1–2 μm) ceramic, domain length is comparable to grain size. The internal stress at the grain boundaries cannot be fully released; even with a much higher 90° domain density, grains and domains are in a clamped condition.¹⁶ The total 90° domain area will increase with the square root of inverse of grain

size when grain size is smaller than 10 μm (90° domain area is almost constant at a grain size larger than 10 μm)⁹ though the domain width decreases with reducing grain size. The steep increase in dielectric constant in the ferroelectric phase in fine grain ceramic is attributed to this increased 90° domain area as the contributions to dielectric constant have one component from the domain wall vibration, which is called orientational polarization (the other component comes from the lattice vibration, which is called ionic polarization.¹⁷ KNbO₃ is in orthorhombic phase below 224 °C (Ref. 18) and has a larger unit cell volume, about twice that of barium titanate at room temperature. Doping KNbO₃ thus introduces compression stress. The more KNbO₃ concentration, the higher internal stress introduced, and hence the higher dielectric constant in the ferroelectric state in 3% KNbO₃-BaTiO₃ than 2% KNbO₃-BaTiO₃ with comparable grain size and density.

The shifts of transition temperatures, broader dielectric constant peak, and broadened and smeared internal friction peak and reduced elastic softening (see Fig. 5) in the vicinity of the Curie point in the fine grain ceramic compared with coarse grain ceramic are understandable: Strain field near the grain boundaries can distort the lattice there from tetragonal into orthorhombic or pseudocubic symmetry. Such stressed volume can account for 22% total volume of a grain in fine

grain ceramic ($1 \mu\text{m}$) but only 7% in coarse grain ceramic ($>10 \mu\text{m}$).¹⁷ Therefore even far below the Curie point, there exists a static transitional structure from orthorhombic/pseudocubic to tetragonal from the grain boundary deep into the grain center lattices. The structural gradient thus broadens and smears the apparent dielectric constant peak in the vicinity of the Curie point, as well as lowers the Curie point, in the fine grain ceramic (small deviation in the present work should be attributed to the composition heterogeneity in different pieces, since the Curie point shift is rather small in theory). Orthorhombic structure has twice as many equivalent polarization directions as tetragonal structure, so it can more effectively release the internal stress by forming more twinning bands,¹⁹ increasing its stability. This fact explains the increase of orthorhombic-tetragonal transition temperature in the fine grain ceramic. An alternative explanation is available: stress and strain field at the grain boundary is the main contribution to transition temperature shift. Orthorhombic-tetragonal transition has shear deformation because of the polarization direction as shear stress exists near the grain boundary [Fig. 7(a)], the strain field there makes orthorhombic phase become more stable and hence increases the orthorhombic-tetragonal transition temperature. The Curie point only has a slight change. This is reasonable because the transition involves tensional strain rather than shear strain.

The structural gradient across the grains broadens and smears the internal friction peak and elastic softening during the transformation. Coupling between the spontaneous strain and order parameters is responsible for the internal friction peak itself. Particulars of the coupling can also contribute to broadening. The macroscopic spontaneous strain arises from the accumulative effect of tilting of the octahedron of each unit

cell; meanwhile, twin band motion can contribute to elastic softening because it will also introduce spontaneous strain. Fine grain ceramic has only one or two simple domain types; whereas coarse grain ceramic has numerous hierarchic structural domains.¹⁶ The moving of the complicated 90° domain walls in coarse grain ceramic will introduce more spontaneous strain. The 180° domain wall moving will not introduce spontaneous strain. The contribution to elastic softening from domain wall moving is a unique character during phase transformations²⁰ as domain walls do not move under external stress in the ferroelastic states.¹³ The order parameters refer to the parameters that can describe the changes (in terms of shape and location) of the lattice with respect to the specified coordinate system during the transformation. In pure BaTiO_3 , tetragonality (c/a) begins to decrease when grain size $<1.5 \mu\text{m}$.⁹ In KNbO_3 doped BaTiO_3 , this threshold grain size could be larger than $1.5 \mu\text{m}$ in view of the reduced Curie point. Reduced tetragonality will require less deformation of the unit cell to transform from one phase to another, resulting in reduced order parameters. The effective coupling between spontaneous strain and order parameters is thus weakened in fine grain ceramic with reduced macroscopic strain and order parameters.

Oblique tension and compression in domains near the grain boundary can give rise to positive or negative contributions to the modulus as follows. The domain structure in a fine grain has been illustrated in Fig. 7(a) following Ref. 9. The grain boundary experiences compression and tension stress. The 90° domain can be modeled in a configuration as illustrated by Fig. 7(b). Spring constants k_1 and k_2 are the same. In a relaxed (coarse grain situation) or somewhat unrelaxed (fine grain situation) condition, k_1 and k_2 are fixed in place by the constraint of k_3 . This constraint comes from the

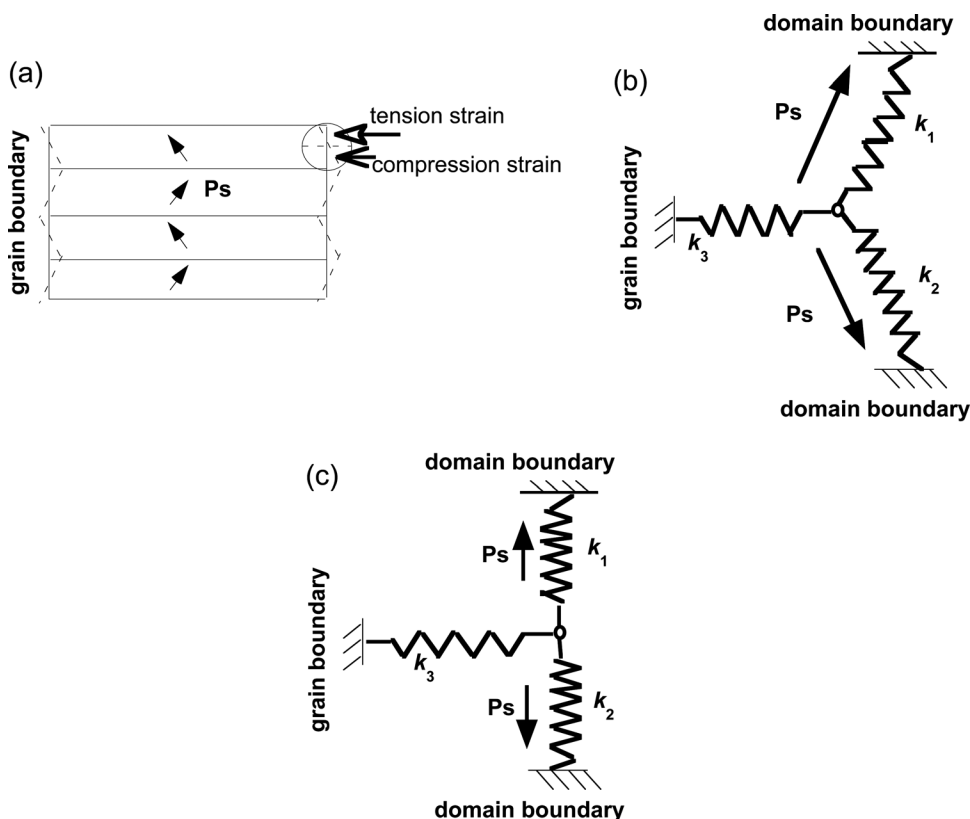


FIG. 7. (a) Schematic domain structure in a fine grain (after Ref. 9). The stress free condition is illustrated by dotted lines. The grain boundary experiences both compression strain and tension strain. (b) 90° domain model in the inner part of the grain or at the grain boundary with free constraint (that is, coarse grain situation). The system is stable due to constraint from k_3 . (c) Domain configuration near the grain boundary in fine grain ceramic. k_1 and k_2 are in a situation entailing snap-through if without k_3 constraint.

grain or domain boundaries in real material. During transformation, the domain switches (which is the macroscopic phenomenon of the tilting of octahedrons). Due to the stress field near the grain boundary, the domain structure there should be very close to the configuration shown in Fig. 7(c). If there is no constraint at the triple point, this point will snap through, causing negative stiffness behavior.³ However, in the presence of stress field near the grain boundary, such a snap through will be restricted. That will stiffen this region due to the constrained negative stiffness effect. As a result, the elastic softening in fine grain ceramic is smeared by this effect. Actually such an effect could exist far below the Curie point near the grain boundary in fine grain ceramic.

The liquid phase layer is formed during sintering due to the existence of unreacted KNbO₃ (melting point 1050 °C) and possible low melting point compounds (BaTi)_x(KNb)_{1-x}O₃ formed during calcinations. Complete diffusion at elevated temperature can gradually exhaust this liquid layer but that will require an extremely long soaking time, which is not practical. The incomplete diffusion results in the core-shell structure for the grains, and thus the lattice structures from the grain boundary deep into the grain center will have a transitional gradient from orthorhombic (pure KNbO₃ is in orthorhombic phase within the temperature range accessed in the present study) to tetragonal at room temperature even without the grain size and constrained negative stiffness effects discussed in the preceding text. However, this effect will be gradually eliminated over multiple ball milling and sintering processes.

The dielectric response in doped ceramic, as mentioned in the preceding text, is much more sensitive to composition heterogeneity in the vicinity of the Curie point (Figs. 1 and 2) than at other temperatures. Such an effect can be explained as follows. At kilohertz driving frequency, the main contribution to dielectric constant comes from the relaxation polarization of various dipoles. Dipoles vibrate around their equilibrium positions in a state of disorder. However, such a movement will be restricted by the interactions with surrounding particles; therefore, the system is in an ordered state before entering the transformation temperature region. When the Curie point is approached, the interactions between dipoles are weakened due to the phonon mode softening and structural relaxation (that is, spontaneous strain); individual dipoles free of constraint could thus be polarized to possess a higher magnitude under the external alternative electric field, enhancing the dielectric response. With increasing sintering cycles, the KNbO₃ layer at the grain boundaries will gradually diffuse into the grain centers, reacting with BaTiO₃. The substitution of K⁺ into Ba²⁺ site is known to introduce Ti³⁺-V_O-K (Ref. 21) type of defect. The drastic increase in the dielectric response near the Curie point in the samples that have experienced more sintering cycles is considered to be the contribution of the increased new types of dipoles introduced by such Ti³⁺-V_O-K defect centers. However, the contribution of these extra dipoles due to the existence of Ti³⁺-V_O-K to dielectric response is not prominent during the lower symmetry phase transformations. The orthorhombic-tetragonal (also orthorhombic-rhombohedral) transition transforms the polarization state of the system from one order to another; the system will not experience a disordered state during the transformation

and will transform into the next ferroelectric state by a shear strain. Therefore, the dipoles will still be under constraint from the lattice during these lower temperature transformations and will not increase the dielectric constant too much under alternating electric field.

V. CONCLUSION

In conclusion, fine grain and coarse grain ceramics sintered at different temperatures exhibit peaks in dielectric constant and in internal friction at transition temperatures. Doping lowered the Curie point and raised the temperature for the structural transformations between rhombohedral and orthorhombic and broadened the response near the transformations. Dielectric and mechanical responses sharpened with increasing sintering cycles but never became as sharp as in pure barium titanate. Reduction in grain size caused a slight shift in Curie point while the orthorhombic-tetragonal transition shifted to higher temperature. Fine grain ceramic exhibited an increase in the dielectric constant in the ferroelectric state and a smearing of the mechanical anomaly near the transformation. These phenomena are attributed to the internal stress built up at the grain boundaries with decreasing grain size as well as the core-shell structure. Doped ceramic exhibited a relaxation peak due to oxygen vacancy with similar activation energy and relaxation time as the pure material.

ACKNOWLEDGMENTS

Support by the National Science Foundation is gratefully acknowledged.

- ¹T. Jaglinski, D. Kochmann, D. S. Stone, and R. S. Lakes, *Science* **315**, 620 (2007).
- ²L. Dong, D. S. Stone, and R. S. Lakes, *Philos. Mag. Lett.* **90**, 23 (2010).
- ³R. S. Lakes, *Phys. Rev. Lett.*, **86**, 2897 (2001).
- ⁴Y. Avrahami and H. L. Tuller, *J. Electroceram.* **13**, 463 (2004).
- ⁵T. Lee, R. S. Lakes, and A. Lal, *Rev. Sci. Instrum.* **71**, 2855 (2000).
- ⁶B. W. Lee, and K. H. Auh, *J. Ceram. Process. Res.* **2**, 134 (2001).
- ⁷L. Dong, D. S. Stone, and R. S. Lakes, *Phys. Status Solidi B* **248**, 158 (2011).
- ⁸K. Kinoshita and A. Yamaji, *J. Appl. Phys.* **47**, 371 (1976).
- ⁹G. Arlt, D. Hennings, and G. de With, *J. Appl. Phys.* **58**, 1619 (1985).
- ¹⁰R. J. Bratton and T. Y. Tien, *J. Am. Ceram. Soc.* **50**, 90 (1967).
- ¹¹B. Jaffe, W. R. Cook, Jr., and H. Jaffe, *Piezoelectric Ceramics* (Academic, London, 1971).
- ¹²R. B. Perez-Saez, V. Recarte, M. L. No, and J. San Juan, *Phys. Rev. B* **57**, 5684 (1997).
- ¹³L. Chen, X. M. Xiong, H. Meng, P. Lv, and J. X. Zhang, *Appl. Phys. Lett.* **89**, 071910 (2006).
- ¹⁴L. Dong, D. S. Stone, and R. S. Lakes, *Appl. Phys. Lett.* **96**, 141904 (2010).
- ¹⁵B. L. Cheng, M. Gabbay, M. Maglione, and G. Fantozzi, *J. Electroceram.* **10**, 5 (2003).
- ¹⁶G. Arlt, *Ferroelectrics*, **104**, 217 (1990).
- ¹⁷T. Hoshina, K. Takizawa, J. Y. Li, T. Kasama, H. Kakemoto, and T. Tsurumi, *Jpn. J. Appl. Phys.* **47**, 7607 (2008).
- ¹⁸B. T. Matthias and J. P. Remeika, *Phys. Rev.* **82**, 727 (1951).
- ¹⁹M. H. Frey and D. A. Payne, *Phys. Rev. B* **54**, 3158 (1996).
- ²⁰Contribution to elastic softening during phase transformations due to domain wall moving can be estimated by the ratio $[ε_t$ (i.e., theoretical spontaneous strain) $-ε_m$ (i.e., measured spontaneous strain)]/ $ε_m$. $ε_t$ is the total unit cell volume difference between parent and new phases. From the experimental perspective, to infer this information requires the usage of single crystal because grain boundary effects dominate in polycrystals.
- ²¹R. Scharfschwerdt, A. Mazur, O. F. Schirmer, H. Hesse, and S. Mendricks, *Phys. Rev. B* **54**, 284 (1996).